SCANNING VOL. 38, 14–20 (2016)
© Wiley Periodicals, Inc.

The Influence of Voltage Applied Between the Electrodes on Optical and Morphological Properties of the InGaN Thin Films Grown by Thermionic Vacuum Arc

Soner Özen,[1] Volkan Şenay,[1,2] Suat Pat,[1] and Şadan Korkmaz[1]

[1]Department of Physics, Eskişehir Osmangazi University, Meşelik Campus, Turkey
[2]Primary Science Education Department, Bayburt University, Turkey

Summary: The aim of this research is to investigate the optical and morphological properties of the InGaN thin films deposited onto amorphous glass substrates in two separate experiments with two different voltages applied between the electrodes, i.e. 500 and 600 V by means of the thermionic vacuum arc technique. This technique is original for thin film deposition and it enables thin film production in a very short period of time. The optical and morphological properties of the films were investigated by using field emission scanning electron microscope, atomic force microscope, spectroscopic ellipsometer, reflectometer, spectrophotometer, and optical tensiometer. Optical properties were also supported by empirical relations. The deposition rates were calculated as 3 and 3.3 nm/sec for 500 and 600 V, respectively. The increase in the voltage also increased the refractive index, grain size, root mean square roughness and surface free energy. According to the results of the wetting experiments, InGaN samples were low-wettable, also known as hydrophobic. SCANNING 38:14–20, 2016. © 2015 Wiley Periodicals, Inc.

Key words: InGaN thin films, thermionic vacuum arc, surface properties, optical properties, surface free energy

Introduction

Group III nitride compounds belong to a commonly studied class of semiconductor materials and they are used in ultraviolet–blue light-emitting diodes (Verzellesi *et al*., 2013; Verma *et al*., 2014; Zhang *et al*., 2014), lasers (Cosendey *et al*., 2012; Takagi *et al*., 2012), tunable mechanical resonators (Montague *et al*., 2011; Ansari and Rais-Zadeh, 2014), sensors (Chen *et al*., 2015) and solar cells (Dahal *et al*., 2014; O'Mahony *et al*., 2014). Nakamura et al. fabricated the first p-GaN/n-InGaN/n/GaN LEDs in 1993 (Nakamura *et al*., '93) and they took the first step of the invention that allows the white light source. The GaN and $In_xGa_{1-x}N$ are highly efficient light emitters even in samples with relatively high densities of structural defects (Wu *et al*., 2002). A small amount of indium addition to the gallium nitride is essential as gallium nitride without indium does not emit a strong band-to-band emission at room temperature (Mukai *et al*., '99). Having high absorption coefficient at the band edge with good thermal conductivity and corrosion resistance (Moses and Van de Walle, 2010), the InGaN alloy is one of the few materials with a direct wide-bandgap of >2.4 eV. The wide-bandgap materials are required in multiple-junction solar cells to achieve a higher efficiency level above 50% (De Vos, '92; Jampana *et al*., 2010). $In_xGa_{1-x}N$ ($0.1 < x < 0.5$) band gap energy ranges between 1.6 eV and 3.3 eV (Anani *et al*., 2007; Moses and Van de Walle, 2010; Bae *et al*., 2014) while its refractive index varies between 2.2 and 2.8 versus the molar fraction "$0.1 < x < 0.5$" (Laws *et al*., 2001; Anani *et al*., 2007; Bae *et al*., 2014).

Challenges exist in production of nitride compounds due to the noble nature of nitrogen. InGaN thin film growth methods can be given as metal organic chemical vapor deposition (MOCVD) (Nakamura *et al*., '93; Ji *et al*., 2003; Jampana *et al*., 2010; Bae *et al*., 2014), molecular beam epitaxy (MBE) (Browne *et al*., 2012; Jiao *et al*., 2013; Muziol *et al*., 2015), rf magnetron sputtering (Andreev, 2003; Guo *et al*., 2010; Wang *et al*., 2013), metal-organic vapor phase epitaxy (MOVPE) (Oliver *et al*., 2003; Ahl *et al*., 2014). In this research, InGaN thin films were prepared on amorphous glass substrates by the non-reactive thermionic vacuum arc technique. Furthermore, this study presents a new deposition technique for GaN-based solid-state applications (Ekem *et al*., 2008; Özen *et al*., 2015; Pat *et al*., 2015; Şenay *et al*., 2015) by

Address for reprints: Soner Özen, Department of Physics, Eskiehir Osmangazi University, Meelik Campus, Turkey 26480.
E-mail: osoner@ogu.edu.tr

Received 7 May 2015; Accepted with revision 22 June 2015

DOI: 10.1002/sca.21237
Published online 18 September 2015 in Wiley Online Library (wileyonlinelibrary.com).

focusing the effect of the applied voltage between the anode and cathode on the morphological and optical properties of the InGaN thin films grown by thermionic vacuum arc. Transparent glass substrates were selected specifically for optical investigation of the produced films. Keep in mind that many attempts have been made to replace single-crystal substrates for the growth of group-III nitrides with low-cost, large-area materials such as glass.

Experimental Details

The thermionic vacuum arc (TVA) is a plasma assisted thin film deposition technique which generates pure metal and non-metal plasma. It is based on the electron-induced evaporation and does not use a buffer gas such as argon, neon, or helium as some plasma assisted technologies do. The TVA discharge occurs in high or ultra-high vacuum conditions between an externally heated cathode which emits electrons and an anode containing the material to be evaporated. The cathode is a tungsten filament and it is mounted inside an electron-focusing Wehnelt cylinder. The accelerated electrons due to a high dc potential difference (V) applied between the anode and cathode, collide with the anode material. The heated anode material evaporates after some time. During evaporation, discharge current (I_d) occurs between anode and cathode. Very low pressure in the rest of the vacuum chamber allows the atoms to move freely, deposit and condensate on any surface placed in the vacuum chamber. Due to the suitable pressure (P) of vacuum chamber the anode material plasma is deposited on substrate as thin film. The bombardment of the growing film by energetic particles strongly influences the growth mechanisms and the structure of the film leading to a more compact structure and low roughness of the deposited thin layer.

0.2 g of GaN (Alfa Aesar, 99.99%) and 0.03 g of In (Alfa Aesar, 99.99%) pellets were used as the anode materials in tungsten crucibles. The angle between the cathode axis and normal direction to anode surface was fixed at the value of 45° and the distance between the anode and cathode was stably kept at 4 mm in both experiments. The working parameters of the TVA are summarized in Table I. 500 V applied between the electrodes corresponds to the arc ignition voltage of TVA, where the above mentioned conditions allow for ignition of a discharge in the anodic vapor. In order to investigate the effect of a higher voltage than the arc ignition voltage, the other experiment was conducted with 600 V. The thickness values of the growing films were not monitored and controlled during deposition. After the production of the InGaN thin films, the samples were not exposed to any thermal treatment. After samples obtained with 600 V and 500 V of thermionic vacuum arc voltage are called as Sample 1 (S1) and Sample 2 (S2), respectively.

The spectroscopic ellipsometry (SE) is a surface sensitive nondestructive and powerful optical method which is widely used to determine the thickness (d) in the nanometer (nm) range and the optical constants (n and k) of a thin film. The thickness and refractive index values of the produced thin films were determined at an incident angle of 70° using a TT-90 Spectroscopic Ellipsometer. Interferometry can determine thin film characteristics (thickness, refractive index and reflectance) by measuring the amount of light reflected from the thin film over a range of wavelength. This technique has considerable advantages regarding speed and simplicity. The reflectance, refractive index values versus to the wavelength and thickness of InGaN thin films were measured using a Filmetrics F20 device. Uv-Vis spectrophotometry analysis was performed with the incident beam perpendicular to the film surface. Absorbance spectra of the produced films were recorded by a Shimadzu Solid Spec-3700 DUV spectrophotometer in the wavelength range of 300–1500 nm. Atomic force microscopy (AFM) provides information about the growth mechanism, shape and size of grains and roughness of the surface of the sample. Field emission scanning electron microscope (FESEM) analyzes the sample using a focused beam of electrons in the low beam voltage (0.5–2 kV). The surface morphology of the produced film was analyzed by Keysight 8,500 FESEM in secondary electron image mode and Ambios Q-Scope AFM in non-contact mode at ambient condition. Shape and size of grains were determined directly from the taken AFM and FESEM micrographs. ScanAtomic V5.1.0 SPM software to control the AFM was used to obtain the root mean square roughness values. An optical tensiometer measures surface and interfacial tension by analyzing the shape of drop images over time. The contact angle and surface free energy of the produced thin films were investigated by an Attension Theta Lite optical tensiometer. This device uses a source of cold monochromatic LED light and a smooth lighting integration sphere that reduces sample evaporation.

Results and Discussion

A spectroscopic ellipsometer measures the polarization changes that occur upon oblique reflection of polarized light at the surface and it defines standard ellipsometric parameters (psi (Ψ) and delta (Δ)). These standard ellipsometric parameters are related to the polarization changes given below

$$\rho = r_p/r_s = tan\Psi\, e^{i\Delta} \tag{1}$$

where ρ is the complex reflectance ratio, r_p, and r_s are the complex Fresnel's reflection coefficients of the light polarized parallel and perpendicular to the plane of incidence, respectively. Ellipsometric characterization method has an indirect nature and it requires an optical

TABLE I TVA working parameters for InGaN thin film production on glass substrates

Working parameters	Unit		Experiment #1	Experiment #2
Working pressure	torr	P	5×10^{-5}	5×10^{-5}
Voltage	V	V	600	500
Filament current	A	I_f	18	18
Discharge current	A	I_d	0.6	0.6
The distance between crucible and the substrate	cm	d	7	7
Deposition time	sec	t	15	10

model which defines the layer thickness and the optical constants of the film of interest. Cauchy equation is the most widely used equation for this purpose. Cauchy equation for the refractive index is given by

$$n(\lambda) = A_n + B_n/\lambda^2 + C_n/\lambda^4 + \ldots \text{ and } k = 0 \qquad (2)$$

where A_n , B_n, and C_n are the parameters used in Cauchy model. The wavelength dependent refractive index n(λ) and the thickness (d) of the InGaN thin films were determined by curve fitting in the wavelength range between 400 and 1000 nm according to Cauchy model. The Mean Squared Error (MSE) was used to quantify the best match between the generation and the experimental curves. The SE spectra between the generation and experimental data having low MSE values for both samples are presented in Figure 1. In Table II, the thicknesses, MSE values and Cauchy model parameters of InGaN thin films were given.

The thicknesses of the produced InGaN films as obtained from Filmetrics F20 are 44 nm for S1 and 30 nm for S2 in high goodness of fit (GOF = 0.995) value. By considering the thickness values determined by Filmetrics F20 and SE, it can be inferred that the average thicknesses of the samples are about 50 nm for S1 and 30 nm for S2. The deposition rates were calculated as 3.3 nm/sec for S1 and 3 nm/sec for S2 by dividing the thickness by the deposition time. According to this, the increase of the applied voltage between the anode and cathode increased the deposition rate.

Refractive index (n) spectra of InGaN thin films obtained by SE and Filmetrics F20 devices are shown in Figure 2a. According to this figure, the refractive indices of the produced films decrease with the increasing wavelength in the observed wavelength range. The obtained refractive index values are consistent with the molar fraction "$0.1 < x < 0.2$' of the $In_xGa_{1-x}N$ in (Anani *et al.*, 2007), the sharp fall between 400–600 nm in (Laws *et al.*, 2001) and refractive index values between

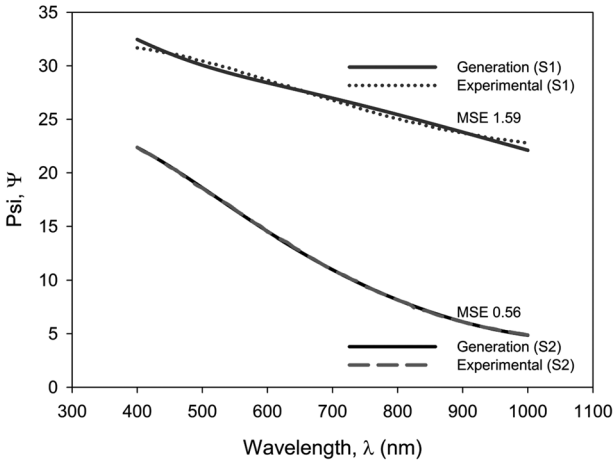


Fig 1. The recorded SE (Ψ) spectra and the generated spectra using the Cauchy dispersion model for produced S1 and S2 thin films.

700–800 nm in (Muziol *et al.*, 2015). The arithmetic refractive index spectra of the Filmetrics F20 and SE refractive index data are seen in Figure 2b. According to this figure, the refractive index changes directly proportional to the voltage applied between the anode and cathode. It is well known that, the refractive index of a material is closely related with its packing density. So, it can therefore be inferred that the S1 sample has a higher packing density than the S2 sample and an increase in the voltage applied between the electrodes enhances the packing density of the produced film.

The absorbance spectra and direct band gap energies determined by optical method of the produced films are presented in Figure 3. The photon absorption resulting with the electron excitation of a valence band electron to the conduction band can be used to determine the optical band gap value. The optical direct band gaps of the InGaN thin films were estimated by optical method using the $(\alpha h\nu)^m$ versus $h\nu$ plots. The direct band gap energies were found to be approximately 2.60 eV for the InGaN thin film with

TABLE II The thickness, model parameters and MSE values of the S1 and S2 thin films deposited on the glass

Material	d (nm) ellipsometry	A_n	$B_n \times 10^{-2}$ (nm^2)	$C_n \times 10^{-2}$ (nm^4)	MSE
S1	54	2.63	−0.57	1.18	1.59
S2	27	2.13	30.11	−2.44	0.56

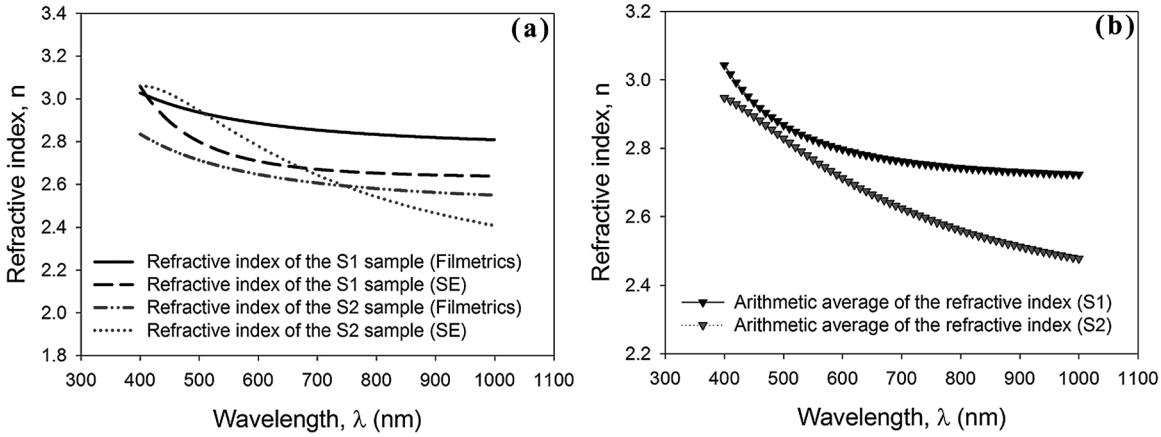


Fig 2. (a) The refractive index spectra, (b) arithmetic refractive index in the Cauchy dispersion model for produced S1 and S2 thin films.

50 nm thickness (S1) and 2.75 eV for the InGaN thin film with 30 nm thickness (S2). Direct band gap values determined by optical method are consistent with the molar fraction "x=0.1' of the $In_xGa_{1-x}N$ in the Moses et al. paper (Moses and Van de Walle, 2010). Band gap energies of the samples are lower than the values reported for GaN thin film on glass substrate in our previous paper (Pat *et al.*, 2015). Indium leads to the shrinkage of the band gap value. According to the energy gap—refractive index relations in semiconductors (Ravindra *et al.*, 2007), this shrinkage will cause an increase in refractive index.

Refractive index and optical band gap values of produced samples were compared using the Moss and Reddy relations. The Moss relation is a simple empirical relationship. This empirical relation between the refractive index and the band gap energy is given by (Moss, '85; Reddy and Ahammed, '95).

$$n^4 E_g = 95. \tag{3}$$

Reddy et al. have proposed an equation for refractive index calculation from optical band gap of materials

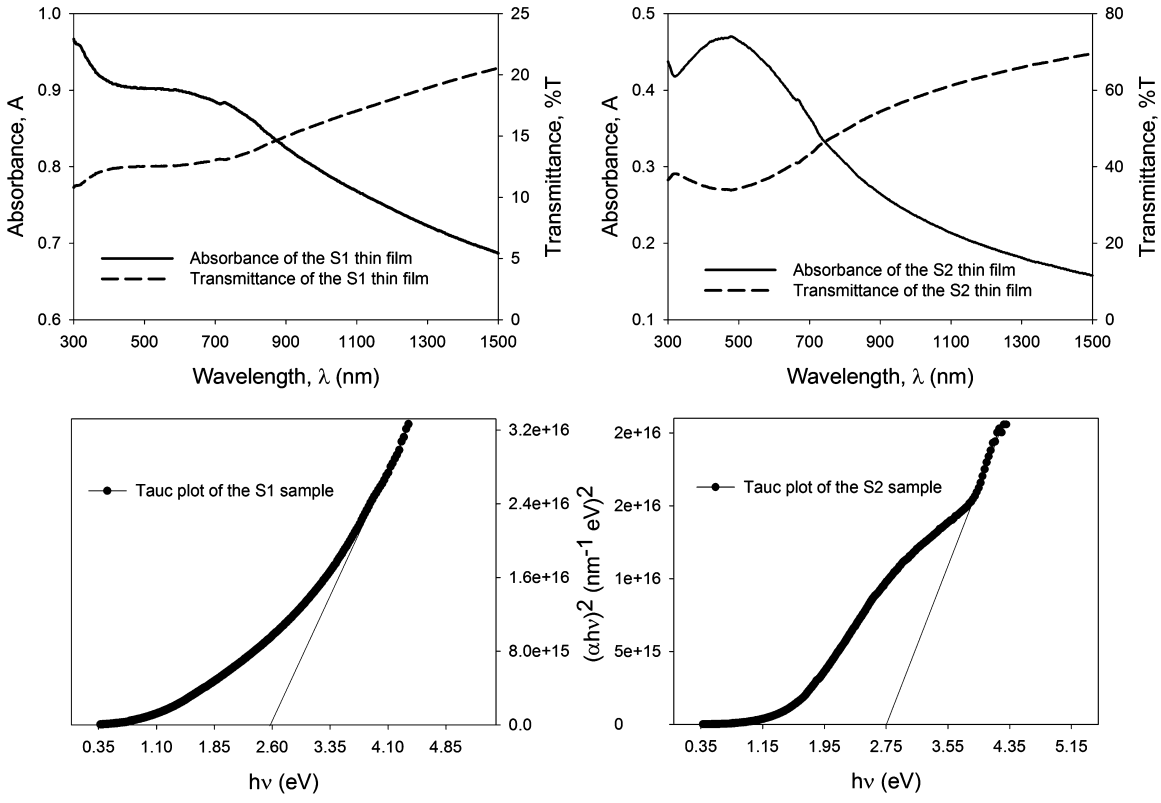


Fig 3. Absorbance graphs and band gap plots of ($\alpha h\nu$) vs. $h\nu$ of the produced InGaN thin films.

(Reddy and Ahammed, '95). This empirical relation is given by

$$n^4(Eg\text{-}0.365) = 154. \quad (4)$$

This equation is a modified form of the original Moss relation. The calculated refractive index values from the band gap values by both empirical relations are presented in Table III. These values show good agreement with literature values (Laws *et al*., 2001; Anani *et al*., 2007; Muziol *et al*., 2015) and the values presented in Figure 2b.

The surface micrographs of the InGaN thin films deposited on the glass substrates are shown in Figure 4.

TABLE III The calculated refractive index values of the S1 and S2 thin films deposited on the glass

Material	Optical band gap value (eV)	Calculated refractive index from moss relation	Calculated refractive index from reddy relation
S1	2.6	2.46	2.88
S2	2.75	2.42	2.83

The photomicrographs revealed that the films were homogenous, nano-structured and granular. Average roughness (Ra) is defined as the average of the individual heights (asperities) and depths from the arithmetic mean elevation of the profile. The average

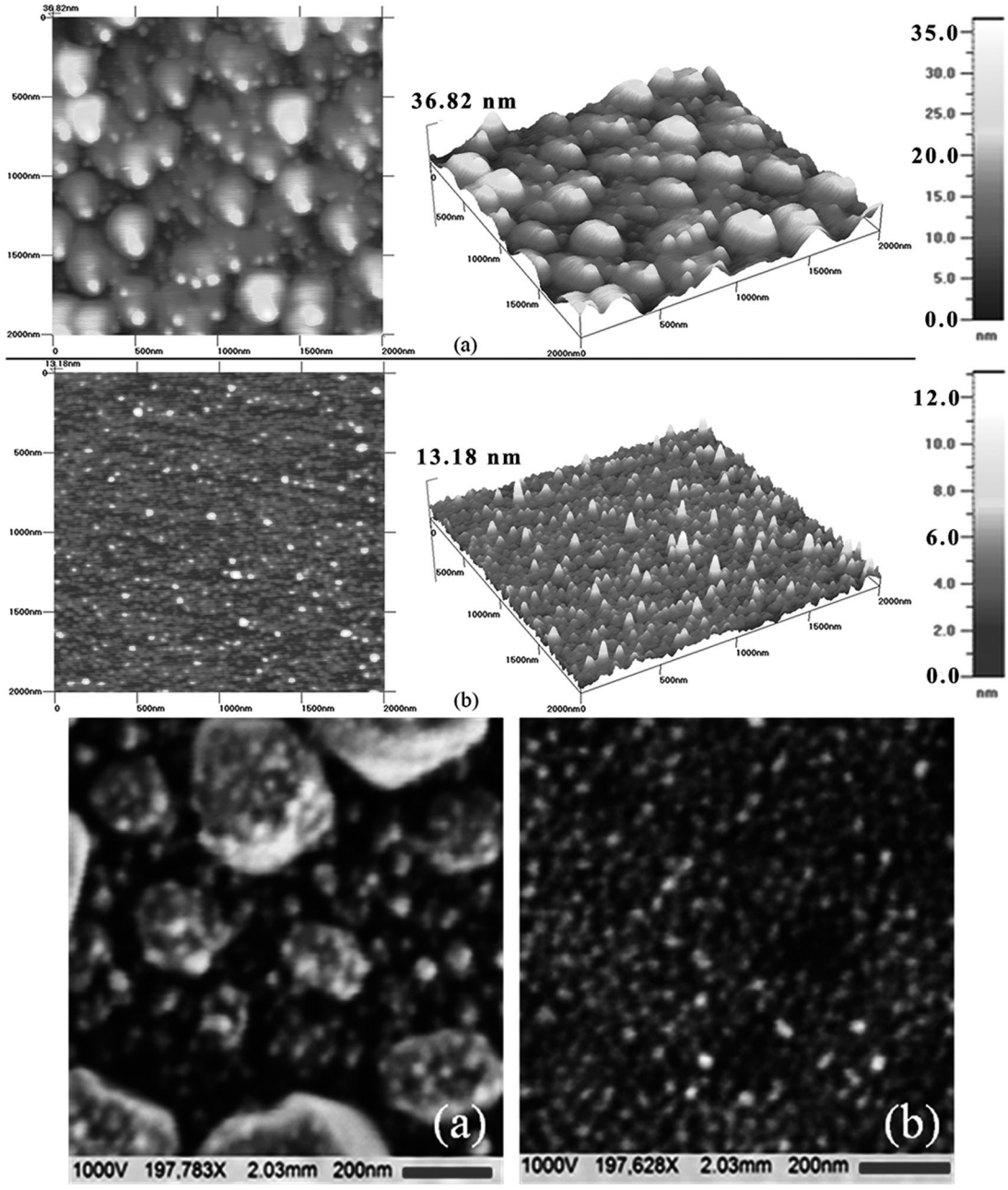


Fig 4. 2D, 3D AFM, and FESEM micrographs of the produced (a) S1 and (b) S2 thin films.

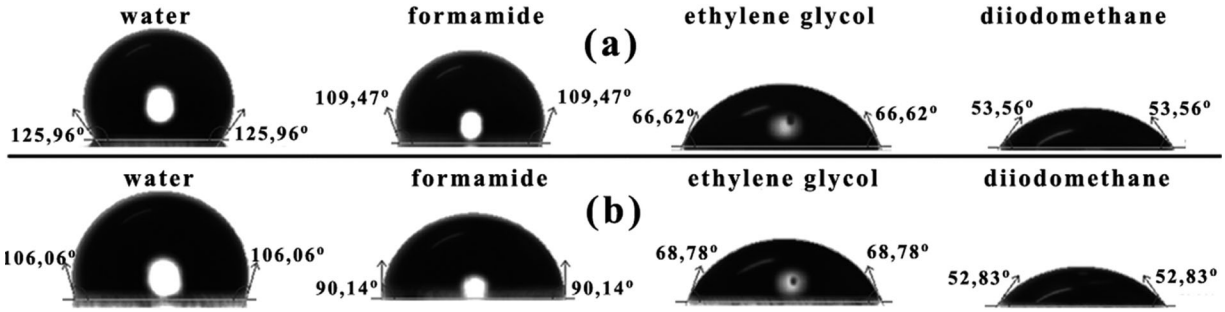


Fig 5. Digital snapshots of four different testing liquid droplets on surfaces of the produced (a) S1, (b) S2 thin films.

roughness values measured with AFM are 4 nm for S1 and 0.8 nm for S2. Root mean square (RMS) roughness is the square root of the sum of the squares of the individual heights and depths from the mean line. The root mean square roughness values are 5 nm for S1 and 1.1 nm for S2. The standard errors of Ra and RMS measurements were determined to be $\pm 5\%$ and %10 for S1 and S2, respectively by the AFM from 7 lines on imaging scale. The nanoparticle largest widths of the produced thin films are approximately 200 nm for S1 and 40 nm for S2 in size. According to the histogram analysis results, average heights of the samples are found to be 13 nm for S1 and 3.5 nm for S2. The increase of applied voltage between anode and cathode increased the average roughness value and grain size of the thin films. In Bae et al. paper (Bae *et al*., 2014), InGaN films were produced on c-plane sapphire substrates with super lattice and grading interlayer. The RMS of the samples are 7.5 nm for the sample with super lattice interlayer and varied between 0.3–2.2 nm for the samples with grading interlayer (Bae *et al*., 2014). Ji et al. proposed that they found circular InGaN quantum dots in diameter of 20–38 nm with an average height of 4 nm from AFM images (Ji *et al*., 2003). The AFM, FESEM micrographs and analysis results found in present study are identical to micrographs and results presented in the literature (Ji *et al*., 2003; Oliver *et al*., 2003; Bae *et al*., 2014). The average roughness and average height presented in (Pat *et al*., 2015) are consistent with S2 sample. S1 sample has higher roughness and larger grains.

The digital snapshots of water, formamide also known as methanamide, ethylene glycol and diiodomethane droplets on the produced thin films are presented in Figure 5. The decrease in particle size due to reduction of the applied voltage has reduced the characteristic of being hydrophobic. There are various methods for the calculation of the surface free energy (SFE) of solids. The SFE of a solid can be studied by measuring contact angle with known liquid(s). The total SFE values were calculated according to the Acid-Base, OWRK/Fowkes, Wu, Equation of State and Zisman Methods and the results are presented in Table IV. According to five different methods, the difference in calculated SFE values of S1 is less than the difference in calculated SFE values of S2. Both of the produced samples showed low wettability.

TABLE IV The total SFE values determined using four different testing liquids

Method	SFE of S1 (mN/m)	SFE of S2 (mN/m)
Acid–base	34.318	31.673
Equation of state	21.249	25.418
OWRK/fowkes	33.166	30.625
Wu	28.486	31.656
Zisman	35.916	31.139

Conclusion

The TVA deposition of InGaN thin films on amorphous glass substrates have been investigated in terms of the effect of the voltage applied between the electrodes on morphological and optical properties. The increase in the voltage increased the refractive index, grain size, RMS roughness and surface free energy. The sample S2 produced at 500 V potential difference has a more uniform structure than the sample S1 produced at 600 V potential difference. From AFM and FESEM micrographs, quantum dots were observed in both of the produced samples. From the refractive index values obtained by SE and interferometry analysis, the Reddy empirical relation was observed to be more compatible than the Moss empirical relation. The average surface free energy values obtained from the employed five different methods are 31 mN/m for S1 and 30 mN/m for S2, indicating low wettability. Finally, it is possible to adjust the physical properties of a thin film grown by TVA technique by changing the voltage applied between the electrodes and implementation of correct voltage is crucial to increase the thin film quality.

References

Ahl J-P, Hertkorn J, Koch H, et al. 2014. Morphology, growth mode and indium incorporation of MOVPE grown InGaN and AlInGaN: a comparison. J Crystal Growth 398:33–39.

Anani M, Abid H, Chama Z, et al. 2007. InxGa 1− xN refractive index calculations. Microelectronics J 38:262–266.

Andreev A. 2003. Intrinsic and Zn-, Ce-, Tb-, Er-, Sm-, and Eu-Activated photoluminescence of pseudoamorphous GaN and InGaN thin films. Phys Solid State 45:419–425.

Ansari A, Rais-Zadeh M. 2014. A thickness-mode AlGaN/GaN resonant body high electron mobility transistor. IEEE Trans Electron Devices 61:1006–1013.

Bae S-Y, Song Y-H, Jeon S-R, et al. 2014. Pseudomorphic thick InGaN growth with a grading interlayer by metal organic chemical vapor deposition for InGaN/GaN p-i-n solar cells. J Crystal Growth 387:23–28.

Browne DA, Young EC, Lang JR, Hurni CA, Speck JS. 2012. Indium and impurity incorporation in InGaN films on polar, nonpolar, and semipolar GaN orientations grown by ammonia molecular beam epitaxy. J Vacuum Sci Technol A 30:041513.

Chen C-C, Chen H-I, Liu I-P, et al. 2015. Enhancement of hydrogen sensing performance of a GaN-based Schottky diode with a hydrogen peroxide surface treatment. Sensors and Actuat B-Chem 211:303–309.

Cosendey G, Castiglia A, Rossbach G, Carlin J-F, Grandjean N. 2012. Blue monolithic AlInN-based vertical cavity surface emitting laser diode on free-standing GaN substrate. Appl Phys Lett 101:151113.

Dahal R, Pantha B, Li J, Lin J, Jiang H. 2014. Realizing InGaN monolithic solar-photoelectrochemical cells for artificial photosynthesis. Appl Phys Lett 104:143901.

De Vos A. 1992. Endoreversible thermodynamics of solar energy conversion. Oxford Univ. Press 52(2):90.

Ekem N, Musa G, Pat S, et al. 2008. Carbon thin film deposition by Thermionic Vacuum Arc (TVA). J optoelectronics and advanced materials 10:672–674.

Guo Q, Kusunoki Y, Ding Y, Tanaka T, Nishio M. 2010. Properties of InGaN Films Grown by Reactive Sputtering. Jpn J Appl Phys 49:081203.

Jampana BR, Melton AG, Jamil M, et al. 2010. Design and realization of wide-band-gap (2.67eV) InGaN pn junction solar cell. Electron Device Lett IEEE 31:32–34.

Ji L, Su Y-K, Chang S-J, et al. 2003. Growth of nanoscale InGaN self-assembled quantum dots. J Crystal Growth 249:144–148.

Jiao W, Kong W, Li J, et al. 2013. The relationship between depth-resolved composition and strain relaxation in InAlN and InGaN films grown by molecular beam epitaxy. Appl Phys Lett 103:162102.

Laws G, Larkins E, Harrison I, Molloy C, Somerford D. 2001. Improved refractive index formulas for the AlxGa1− xN and InyGa1− yN alloys. J Appl Phys 89:1108–1115.

Montague JR, Bertness KA, Sanford NA, Bright VM, Rogers CT. 2011. Capacitive readout technique for studies of dissipation in GaN nanowire mechanical resonators. Am Soc Mech Eng 329–333.

Moses PG, Van de Walle CG. 2010. Band bowing and band alignment in InGaN alloys. Appl Phys Lett 96:021908.

Moss T. 1985. Relations between the refractive index and energy gap of semiconductors. Physica Status Solidi 131:415–427.

Mukai T, Yamada M, Nakamura S. 1999. Characteristics of InGaN-based UV/blue/green/amber/red light-emitting diodes. Jpn J Appl Phys 38:3976.

Muziol G, Turski H, Siekacz M, et al. 2015. Enhancement of optical confinement factor by InGaN waveguide in blue laser diodes grown by plasma-assisted molecular beam epitaxy. Appl Phys Exp 8:032103.

Nakamura S, Senoh M, Mukai T. 1993. P-GaN/N-InGaN/N-GaN double-heterostructure blue-light-emitting diodes. Jpn J Appl Phys 32:L8.

Oliver RA, Briggs GAD, Kappers MJ, et al. 2003. InGaN quantum dots grown by metalorganic vapor phase epitaxy employing a post-growth nitrogen anneal. Appl Phys Lett 83:755–757.

O'Mahony D, Parbrook P, Corbett B, et al. 2014. Spectral analysis of In X Ga 1− x N/GaN quantum well structures for III-nitride based solar cells. In Advanced Semiconductor Devices & Microsystems (ASDAM), 10th International Conference on IEEE 1–3.

Özen S, Pat S, Şenay V, Korkmaz Ş, Geçici B. 2015. Some physical properties of the SiGe thin film coatings by Thermionic Vacuum Arc (TVA). J Nanoelectro Optoelectro 10:56–60.

Pat S, Korkmaz Ş, Özen S, Şenay V. 2015. GaN thin film deposition on glass and PET substrates by thermionic vacuum arc (TVA). Mater Chem Phys 159:1–5.

Ravindra NM, Ganapathy P, Choi J. 2007. Energy gap-refractive index relations in semiconductors-An overview. Infrared Phys Technol 50:21–29.

Reddy R, Ahammed YN. 1995. A study on the Moss relation. Infrared Phys Technol 36:825–830.

Şenay V, Özen S, Pat S, Korkmaz Ş. 2015. Some physical properties of a Si-Doped nano-crystalline GaAs thin film grown by thermionic vacuum arc. Vacuum 119:228–232. DOI: 10.1016/j.vacuum.2015.05.030

Takagi S, Enya Y, Kyono T, et al. 2012. High-power (over 100mW) green laser diodes on semipolar {20$\bar{2}$1} GaN substrates operating at wavelengths beyond 530 nm. Appl Phys Exp 5:082102.

Verma J, Islam S, Protasenko V, et al. 2014. Tunnel-injection quantum dot deep-ultraviolet light-emitting diodes with polarization-induced doping in III-nitride heterostructures. Appl Phys Lett 104:021105.

Verzellesi G, Saguatti D, Meneghini M, et al. 2013. Efficiency droop in InGaN/GaN blue light-emitting diodes: physical mechanisms and remedies. J Appl Phy 114:071101.

Wang J, Shi X, Zhu J. 2013. Low-temperature growth of In x Ga 1− x N films by radio-frequency magnetron sputtering. Appl Surf Sci 265:399–404.

Wu J, Walukiewicz W, Yu K, et al. 2002. Indium nitride: a narrow gap semiconductor. Lawrence Berkeley Nat Lab 9: 1384–1387.

Zhang Q, Li B, Huang S, et al. 2014. Efficient blue organic light-emitting diodes employing thermally activated delayed fluorescence. Nat Photonics 8:326–332.